Rev. Lett. 39, 284 (1977); K. Estabrook and W. Kruer, Phys. Rev. Lett. 40, 42 (1977).
[10]H.-S. Kwok and E. Yablonovitch, Appl. Phys. Lett. 30, 158 (1977).
[11]H. Ahlsmeyer, J. Fluid. Mech. 74, 497 (1976).
[12]E. Yablonovitch, Appl. Phys. Lett. 23, 121 (1973).
[13]H.-S. Kwok, Ph.D. thesis, Harvard University, 1978 (unpublished).

Profile Modification and Hot-Electron Temperature from Resonant Absorption at Modest Intensity

J. R. Albritton and A. B. Langdon
University of California, Lawrence Livermore Laboratory, Livermore, California 94550
(Received 17 April 1980)

Resonant absorption is investigated in expanding plasmas. The momentum deposition associated with the ejection of hot electrons toward low density via wave breaking readily exceeds that of the incident laser radiation and results in significant modification of the density profile at critical density. New scaling of hot-electron temperature with laser and plasma parameters is presented.

PACS numbers: 52.50.Jm

Theory indicates that lasers of current application may be expected to exhibit significant collisionless interaction with inertial-confinement fusion targets. Here we consider resonant absorption[1] which acts at critical density where the laser frequency equals the local electron plasma frequency. Because the dominant laser-plasma coupling occurs near critical density, it is essential to develop a self-consistent description of the dynamics there. It will be seen that even weak resonant absorption acts strongly upon the hydrodynamical evolution of this region so as to enhance itself and suppress other mechanisms.

Resonant electron oscillations transfer absorbed energy to the plasma by ejecting particles toward low density via wave breaking.[1] *The associated momentum deposition readily exceeds that of the driving laser radiation.* These hot collisionless electrons are confined by the electrostatic potential and subsequently pose two challenges to laser fusion: (1) to prevent them from preheating the target and (2) to use their energy to drive its implosion.

Implosion experiments at *modest* intensity are already in progress[2] to increase the density of the compressed core above that of *high*-intensity exploding-pusher target experiments[3] which are strongly preheated by hot electrons from resonant absorption. The scaling of hot-electron temperature in the high-intensity regime is the subject of recent theoretical work[4,5]; briefly, the laser beam or driven wave steepens the density profile at critical density and thereby reduces the rate of increase of the hot-electron temperature with increasing laser intensity from estimates based on the usual coronal rarefaction.

Here we report new and improved scaling laws for the temperature of hot electrons produced by resonant absorption in the modest intensity regime. (We will, in fact, argue for the general validity of our results.) *The dependence of hot-electron temperature upon background cold-electron temperature is shown to be as strong as that upon laser intensity.*

The interaction of modest-intensity 1.06-μm laser radiation with high-Z disc targets has been modeled by *ad hoc* strong limitation of electron energy conduction.[6] The resulting coronal rarefaction exhibits a step in density including critical and hot plasma below the subcritical density at which the flow emerges from the step. Most interaction mechanisms are suppressed in such a profile.

In fact, resonant absorption is enhanced in a self-consistent stepped density profile.[1,4,5,7] *Here we provide a first principles model of profile modification in the modest-intensity regime as the local response of the flow to the momentum deposited at critical density by hot-electron production.*

The upper density of the induced step may be much greater than critical density and much greater than that associated with radiation-pressure steepening. Experimental observations of such structures have been reported recently.[8] The associated lower density and absence of an extensive turning region act to suppress inverse bremsstrahlung and stimulated Brillouin scattering. The step in electrostatic potential associated with the density step contributes to the formation

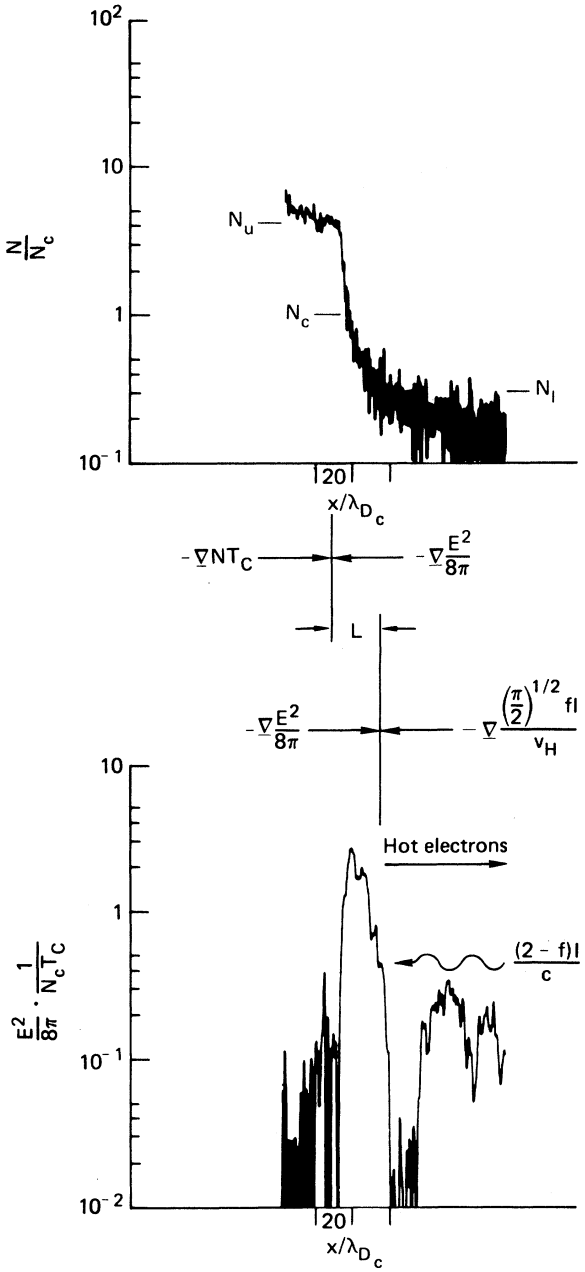

FIG. 1. The density profile and electrostatic field energy density associated with resonant absorption in an expanding plasma. The curves are simulation data for $v_0/v_c=1$ at $t=1200/\omega_0$; $\omega_0=\omega_{p,\max}/5$.

of a hot corona since electrons sufficiently energetic to climb it may be expected to possess an elevated temperature as well.

Here we describe a study performed with the one-dimensional, electrostatic, particle simulation code ES1[9] to investigate the scaling of energy, momentum, and charge balance of resonant absorption in the modest-intensity regime, defined as that in which the driven-wave pressure dominates the laser-radiation pressure. Thus the laser is seen to contribute primarily energy to the system while in the high-intensity regime it contributes both energy and momentum.

The essential physical notion here is that the system relaxes locally such that the sharply peaked energy density or ponderomotive pressure of the resonant wave is balanced on the overdense side by the background plasma pressure and on the underdense side by the reaction to the momentum flux of hot electrons ejected toward the vacuum. The critical-density region and driven resonant wave is shown in Fig. 1. From consideration of pressure balance on the underdense side of the wave, we estimate $E^2/8\pi\sim(\pi/2)^{1/2}fI/v_h$.[10] Here f is the absorption fraction of laser intensity I into hot electrons of velocity $v_h=(T_h/m)^{1/2}$.

The momentum flux of hot electrons exceeds that of the laser radiation whenever $(\pi/2)^{1/2}fI/v_h>(2-f)I/c$, or

$$T_{h,\text{modest}}<(511\pi/2)f^2/(2-f)^2\ \text{keV}. \quad (1)$$

Experience indicates that 0.3 is a useful estimate for f; Eq. (1) then becomes $T_{h,\text{modest}}<25$ keV, and the modest-intensity regime in the laboratory is found to be[11] $I(\text{W/cm}^2)\lambda^2(\mu\text{m})_{\text{modest}}<10^{16}$.

From consideration of momentum balance on the overdense side we estimate $-\nabla(NT_c)\sim-\nabla(E^2/8\pi)\sim-\nabla(\pi/2)^{1/2}fI/v_h$ so that by crude integration the upper density associated with resonant absorption, N_u^*, is

$$N_u^*/N_c\sim1+(\pi/2)^{1/2}fI/N_cT_cv_h. \quad (2)$$

For the experimental parameters of Ref. 8 this steepening is more than three times that associated with the radiation pressure!

In general the radiation-pressure contribution should be included in estimating the upper density. However, an upper density greater than that given in Eq. (2) may be expected not to change the dynamics of the driven resonant wave qualitatively from that described here. The longer scale length ($\sim c/\omega_p$) over which the radiation pressure acts suggests a doubly stepped profile in which the resonant wave dominates locally but where the maximum density may be determined by radiation pressure. In this picture our results may be extended to the high-intensity regime.

Our simulation code evolves the dynamics of an initially uniform slab of electrons and ions which

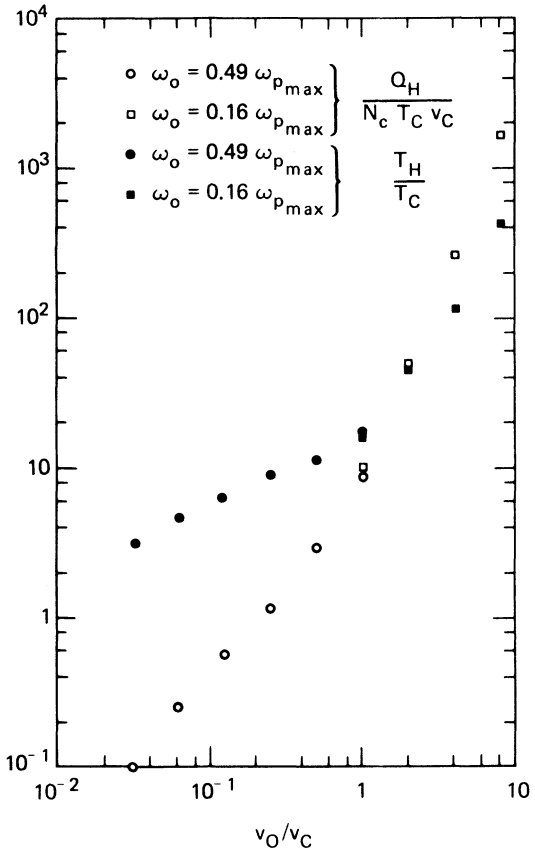

FIG. 2. The hot-electron temperature, T_h, and the hot-electron heating rate, Q_h, increase with increasing pump strength, v_0. Note the different scalings which obtain in the regimes of warm dynamics, $v_0/v_c < 1$, and cold dynamics, $v_0/v_c > 1$.

expand into vacuum under the influence of a high-frequency capacitor-model[1] pump. By mapping the hot-electron heating rate onto absorbed laser intensity[1] we will cast our results into a form useful for laboratory application[12] and comparison to electromagnetic simulations.[1,4,5]

The driven systems are characterized by the single dimensionless parameter, v_0/v_c, where $v_0 = eE_0/m\omega_0$ is the jitter velocity of an electron in the pump field, and $v_c = (T_c/m)^{1/2}$ the initial (cold) electron thermal velocity ($T_c/T_i \sim 3$, $m/M \sim \frac{1}{900}$). Even for v_0/v_c less than $(m/M)^{1/2}$ we find that wave breaking governs the system: Neither convection nor solition formation have been seen. Our principal results are the variation with v_0/v_c of the hot-electron temperature, the hot-electron heating rate, and the densities delimiting the step.

In Fig. 2, the normalized hot-electron temperature, T_h/T_c, and the normalized hot-electron heating rate, $Q_h/N_c T_c v_c$, are plotted against v_0/v_c. Note the break in the slope of the data at $v_0/v_c \sim 1$. *Cold* plasma modeling is appropriate for $v_0/v_c > 1$ while $v_0/v_c < 1$ is the *warm* plasma regime.

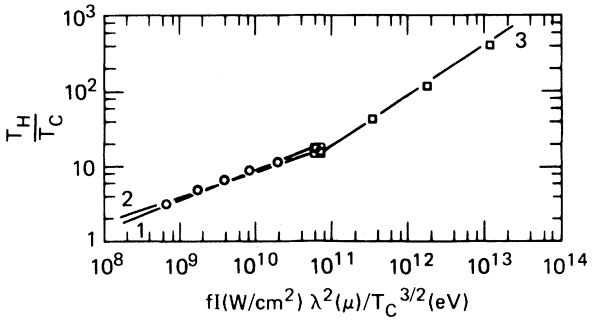

FIG. 3. Identifying the hot-electron heating rate, Q_h, with absorbed laser intensity, fI, the two curves in Fig. 2 are combined to obtain the scaling of T_h with the laboratory observables f, I (W/cm^2), $\lambda^2(\mu$m), and T_c (eV). Curve 1, with slope $\frac{2}{5}$, curve 2, with slope $\frac{1}{3}$, and curve 3, with slope $\frac{2}{3}$, are discussed in the text.

Let us now identify the hot-electron heating rate with absorbed laser intensity. We have $Q_h/N_c T_c v_c$ and T_h/T_c as functions of v_0/v_c; we identify $Q_h = fI$ and then eliminate v_0/v_c to obtain the data displayed in Fig. 3. Note the role played by the background temperature as T_h/T_c varies against $fI(\mathrm{W/cm^2})\lambda^2(\mu\mathrm{m})/T_c^{3/2}(\mathrm{eV})$. In the warm-plasma limit $fI\lambda^2/T_c^{3/2} < 10^{11}$ we have drawn lines with slopes of $\frac{2}{5}$ and $\frac{1}{3}$. These yield the preferred scaling, $T_h(\mathrm{eV}) = 9\times10^{-4}(fI\lambda^2 T_c)^{2/5}$, which compares favorably with that given in Ref. 5, or, still within confidence limits, $T_h = 4\times10^{-3}(fI\lambda^2)^{1/3}T_c^{1/2}$, which compares favorably with that given in Ref. 4. Note that the scaling with cold background temperature is as strong as that with intensity. The cold-plasma limit given in Ref. 12 is recovered for $fI\lambda^2/T_c^{3/2} > 10^{11}$, where $T_h = 9\times10^{-7}(fI\lambda^2)^{2/3}$ independent of T_c.

Comparison of our results with the data of Giovanelli[12] suggests that the interaction in the laboratory is governed by cold-plasma dynamics for $I\lambda^2 < 10^{15}$ where the $\frac{2}{3}$ power obtains ($T_h/T_c = $ const leads to the same scaling) and warm-plasma dynamics for $I\lambda^2 > 10^{15}$ where the $\frac{2}{5}$ or $\frac{1}{3}$ power obtains.

The $\frac{2}{3}$-power scaling of hot-electron temperature was suggested previously by flux-limit and stochastic-heating estimates.[13] Let us briefly recapitulate the cold-plasma estimates for resonant absorption which yield the $\frac{2}{3}$-power scaling[11] confirmed here. Wave breaking occurs when elec-

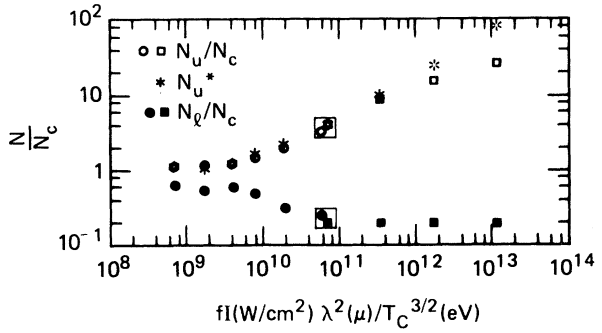

FIG. 4. The upper, N_u, and lower, N_l, densities delimiting the step at critical density, N_c, increase and decrease, respectively, with increasing pump strength. The estimated upper density, N_u^* of Eq. (2), is in agreement with observations except in the most strongly driven systems.

trons oscillate in the wave with a velocity, $v_e \sim eE/m\omega$, which scales with the effective phase velocity of the wave $v_e \propto v_p \sim L/(2\pi/\omega)$. The hot-electron temperature scales with the energy an electron can gain in riding the wave across the resonant region, $T_h \propto eEL$. Combining these we find $E^2/8\pi \sim N_c T_h/4\pi$. Recall that momentum balance on the underdense side of the wave requires $E^2/8\pi \sim (\pi/2)^{1/2} fI/v_h$. Combining again yields $T_h \propto (fI\lambda^2)^{2/3}$, exactly the desired result.

Finally in Fig. 4 we show the upper and lower densities bounding the step at critical, N_u/N_c and N_l/N_c, respectively, and the estimated upper density, N_u^*/N_c, as functions of $fI\lambda^2/T_c^{3/2}$. The agreement of the estimated upper density is quite good except for the strongest pumps—neglect of the flow contribution to momentum balance in the step region[1,7] may be the major source of error. Typical values of the lower density are seen to be less than half the critical density.

We gratefully acknowledge E. I. Thorsos, E. A. Williams, and W. L. Kruer for their contributions to this work. This work was supported by the U.S. Department of Energy under Contract No. W-7405-ENG-48.

[1]J. P. Friedberg, R. W. Mitchell, R. L. Morse, and L. I. Rudsinski, Phys. Rev. Lett. 28, 795 (1972); P. Koch and J. Albritton, Phys. Rev. Lett. 32, 1420 (1974), and Phys. Fluids 18, 1136 (1975); K. Estabrook, E. J. Valeo, and W. L. Kruer, Phys. Lett. 49A, 109 (1974), and Phys. Fluids 18, 1151 (1975); J. S. DeGroot and J. E. Tull, Phys. Fluids 18, 672 (1975); D. W. Forslund, J. M. Kindel, K. Lee, E. L. Lindman, and R. L. Morse, Phys. Rev. A 11, 679 (1975).

[2]W. C. Mead *et al.*, UCRL Report No. UCRL-813163, 1979 (unpublished).

[3]W. C. Mead *et al.*, UCRL Report No. UCRL-80006, 1977 (unpublished).

[4]D. W. Forslund, J. M. Kindel, and K. Lee, Phys. Rev. Lett. 39, 284 (1977).

[5]K. Estabrook and W. L. Kruer, Phys. Rev. Lett. 40, 42 (1978).

[6]M. D. Rosen *et al.*, Phys. Fluids 22, 2020 (1979).

[7]D. W. Forslund, J. M. Kindel, K. Lee, and E. L. Lindman, Phys. Rev. Lett. 36, 35 (1976).

[8]R. Fedosejevs, M. D. J. Burgess, G. D. Enright, and M. C. Richardson, Phys. Rev. Lett. 43, 1664 (1979).

[9]C. K. Birdsall and A. B. Langdon, *Plasma Physics via Computer Simulation* (Univ. California Press, Berkeley, 1975).

[10]The factor $(\pi/2)^{1/2}$ results from employing a one-dimensional half-Maxwellian distribution in computing the hot-electron momentum flux in terms of its energy flux.

[11]J. R. Albritton, E. I. Thorsos, and E. A. Williams, Laboratory for Laser Energetics, University of Rochester, Report No. 85, 1978 (unpublished).

[12]D. V. Giovanelli, Report No. LA-UR 76-2242, 1976 (unpublished); K. R. Manes *et al.*, J. Opt. Soc. Am. 67, 717 (1977).

[13]R. L. Morse and C. W. Nielson, Phys. Fluids 16, 909 (1973).